Therefore, our energy-selective intensity measurements were made to choose a positive-peak position of the dispersive XMCD, which locates in a wavelength of λ = 1.7442 Å (*E* = 7.1082 keV).

The synchrotron experiments on RXMS of magnetite were performed with a Rigaku AFC5 four-circle diffractometer in Photon Factory BL-6C, where monochromatized X-rays are reproduced with the circularly polarization by a diamond (001) phase retarder. A spherical crystal of 0.13 mm in diameter was mounted along the a_3 axis on the glass fiber on a rare-earth magnet. The crystal was grown from Fe_3O_4 powder in Pt-10 % Rh crucible by the Bridgman method in the CO-CO_2 atmosphere and provided by Drs. S. Todo and H. Kawata. The cell dimension is a = 8.4000(3) Å (*s.g. Fd*-3*m*). At temperatures of T = 125, 200 and 300 K, integrated intensity data were collected at a scan speed of 0.5 °/min in ω. A total of 425 reflections was collected within the range of $2\theta \leq 100°$ and $-7 \leq h, k, l \leq 7$ and corrected for the angle-dependent polarization effect. Intensity difference ($I^+ - I^-$) between left- and right-circular polarizations extracts the RXMS effect and is roughly proportional to the real part of $F^*_{charge}F_{spin}$ in complex conjugation of crystal structure factors.

Difference-Fourier maps on targeted magnetic electrons were sybthesized from the F difference between left- and right-circular polarizations. With some replacements of calculated F_{calc} for observed one, the usual difference-Fourier formalism can be used for the difference in the electron density of $[\Delta\rho_{obs}(\boldsymbol{r})^{left} - \Delta\rho_{obs}(\boldsymbol{r})^{right}]$ [4]. Nonessential effects such as charge scattering and experimental errors can be cancelled out in the difference-Fourier synthesis. Thus, in this study difference-Fourier maps of magnetite were obtained as a function of temperature and will be discussed for the magnetic electron density at the electronic transition energy so far examined. Our results show that the appearance of positive and negative peaks are caused by magnetic unpaired 3*d* electrons around Fe atoms associated with neighboring oxygen and the other Fe atoms. It suggests the existence of the A-O-B super exchange interaction.

[1] K. Namikawa, M. Ando, T. Nakajima, H. Kawata, *J. Phys. Soc. Jpn.* **1985**, *54*, 4099-4102. [2] J.P. Hannon, G.T. Trammell, M. Blume, D. Gibbs, *Phys. Rev. Lett.* **1988**, *61*, 1245-1248. [3] P. Carra, M. Altrarelli, F. Bergevin, *Phys. Rev. B* **1989**, *40*, 7324-7372. [4] Y. Kaneko, M. Okube, S. Sasaki, *Am. Inst. Phys. Conf. Proc.* **2010**, *1234*, 871-874.

Keywords: resonant_magnetic_scattering, electron_density, iron_oxide

MS48.P03

Acta Cryst. (2011) A**67,** C530

Magnetic structures of $BaTiMFe_{10}O_{19}$ (M = Mn, Co) by resonant magnetic scattering

Atsushi Kinoshita,[a] Maki Okube,[b] Takeshi Toyoda,[c] Satoshi Sasaki,[b]
[a]*Interdisciplinary Graduate School of Science and Engineering, Tokyo Institute of Technology, Yokohama (Japan).* [b]*Materials and Structures Laboratory, Tokyo Institute of Technology, Yokohama (Japan).* [c]*Industrial Research Institute of Ishikawa, Kanazawa (Japan).* E-mail: kinoshita.a.ac@m.titech.ac.jp

The magnetic structures of *M*-type $BaTiMFe_{10}O_{19}$ (M = Mn, Co) have been determined by the resonant X-ray magnetic scattering (RXMS) method [1-4], where the spin-orbit coupling gives magnetic resonance at the *K* edge through the superexchange interaction between 4*p* and 3*d* sates with 2*p* of oxygen atoms. Although barium hexaferrite $BaFe_{12}O_{19}$ has the strong uniaxial anisotropy in magnetization along *c* axis, the substitution of Fe^{3+} by Ti^{4+}/M^{2+} results in a weakening of the magnetic interactions. The structure analyses based on neutron diffraction [5] and RXMS [4] measurements have suggested that Ti^{4+}/Co^{2+}-substituted crystals have ferrimagnetic structures with the canting of the magnetic moments. It is considered that the array of magnetic moments among five cation sites is different between Ti^{4+}/Mn^{2+} and Ti^{4+}/Co^{2+} substitutions.

Synchrotron X-ray intensity measurements were made for single crystals of ferrimagnetic ferrites at BL-6C of the Photon Factory. X-ray magnetic circular dichroism (XMCD) and RXMS effects were examined with intensity differences between the right- and left-circular polarizations, produced by a transmission-type phase retarder of diamond (001). The XMCD measurements are important to pinpoint the photon energy required for RXMS, where a negative XMCD signal around E = 7.123 keV has a chemical shift between Ti^{4+}/Mn^{2+} and Ti^{4+}/Co^{2+} ferrites. By using a Rigaku AFC5 four-circle diffractometer, intensity measurements of RXMS for $BaTiMnFe_{10}O_{19}$ and $BaTiCoFe_{10}O_{19}$ were made in an ω–2θ scan mode at wavelengths of λ = 1.7402 Å (*E* = 7.1245 keV) and 1.7406 Å (7.1228 keV) at the Fe *K* edge, respectively.

Single crystals of ferrites were grown by a flux method. The crystal symmetry is hexagonal with the space group $P6_3/mmc$ and cell dimensions are a = 5.9039(2) and c = 23.2047(8) Å for Ti-Mn and a = 5.8955(3) and c = 23.205(2) Å for Ti-Co. The crystal structure can be built up with a sequence of spinel *fcc* blocks of $(Fe_6O_8)^{2+}$ and *hcp* blocks of $(BaFe_6O_{11})^{2-}$. Five independent Fe sites exist as tetrahedral $4f_1$, bipyramidal 2*b* and three octahedral sites of 2*a*, $4f_2$ and 12*k*. The cation distributions of the barium ferrites have been estimated from single-crystal X-ray diffraction data [6]. Spin orientations were estimated in the least-squares method based on an asymmetrical ratio $\Delta R = (I^+ - I^-)/(I^+ + I^-)$, where I^+ and I^- are left- and right-circular polarized intensities, respectively. The degree of the spin canting for $BaTiMnFe_{10}O_{19}$ was determined in the least-squares calculations with resonant magnetic scattering factors, which was compared with that of $BaTiCoFe_{10}O_{19}$ in the relation between magnetic helices and cation substitution.

[1] K. Namikawa, M. Ando, T. Nakajima and H. Kawata, *J. Phys. Soc. Jpn.* **1985**, *54*, 4099-4102. [2] J.P. Hannon, G.T. Trammell, M. Blume, D. Gibbs, *Phys. Rev. Lett.* **1988**, *61*, 1245-1248. [3] P. Carra, M. Altrarelli, F. Bergevin, *Phys. Rev. B* **1989**, *40*, 7324-7372. [4] M. Okube, Y. Kaneko, S. Ohsawa, T. Toyoda, T. Mori, S. Sasaki, *Am. Inst. Phys. Conf. Proc.*, **2010**, *1234*, 871-874. [5] J. Kreisel, H. Vincent, F. Tasset, m. Paté, J.P. Ganne, *J. Magn. Magn. Mater.* **2001**, *224*, 17-29. [6] Y. Ishida, T. Nakanishi, T. Toyoda, M. Okube, S. Sasaki, *Acta Crystallogr. A (Supplements),* **2008**, *64*, C511.

Keywords: resonant_magnetic_scattering, magnetic_structure, barium_ferrite

MS48.P04

Acta Cryst. (2011) A**67,** C530-C531

X-ray magnetic diffraction and magnetic compton scattering of Pd-Co and Pt-Fe

Masahisa Ito,[a] Ayako Sato,[a] Ryutaro Yamaki,[a] Masahiro Naito,[a] Kojiro Kobayashi,[b] Tatsuya Nagao,[a] Kosuke Suzuki,[a] Hiroshi Sakurai,[a] Hiroshi Maruyama,[c] Masayoshi Itou,[d] Yoshiharu Sakurai,[d]
[a]*Graduate School of Engineering, Gunma University, Kiryu (Japan).* [b]*Advanced Technology Research Center, Gunma University, Kiryu (Japan).* [c]*Graduate School of Science, Hiroshima University, Higashi-hiroshima (Japan).* [d]*JASRI/SPring-8, Nishi-harima, Hyogo (Japan).* E-mail: itom_phys@gunma-u.ac.jp

X-ray magnetic diffraction (XMD) experiment has been performed for Cu_3Au-type single crystal alloys of disordered Pd_3Co and ordered Fe_3Pt, and magnetic Compton scattering (MCS) experiment has been performed for Pd_3Co. The aim of this study is to estimate spin and orbital magnetic moments of the alloys. Electron probe micro analysis (EPMA) has shown that precise chemical composition of Pd_3Co is $Pd_{3.2}Co_{0.8}$. The XMD and MCS experiment were made on BL3C of

KEK-PF and BL08W of SPring-8, respectively. EPMA analysis was made at Center for Material Research by Instrumental Analysis in Gunma University.

The spin and orbital magnetic form factors of $Pd_{3.2}Co_{0.8}$ and Fe_3Pt were measured by the XMD for nearly twenty reciprocal lattice points, and the magnetic Compton profile (MCP) of $Pd_{3.2}Co_{0.8}$ was obtained for three directions along the principal axes [100], [110] and [111].

The observed spin and orbital magnetic form factors were fitted with atomic-model theoretical form factors based on the dipole approximation in order to obtain the spin and orbital magnetic moment of each constituent atom of the alloys. Theoretical form factors for 3d elements of Co and Fe and 4d element of Pd were quoted from the literature [1]. Those for 5d element of Pt were calculated by the authors (K.K. & T.N.) as they were not presented in literatures. The observed MCPs have provided information about the spin moment and directional anisotropy of the momentum distribution of electrons with spin.

The experimental results are as follows. (1) Sum of the spin and orbital moment of $Pd_{3.2}Co_{0.8}$ by the XMD ($2.3\mu_B$ and $0.8\mu_B$, respectively) is $3.1\mu_B$, which is consistent with the magnetic moment $3.16\mu_B$ observed by the magnetization measurement. (2) The estimated spin moment of $Pd_{3.2}Co_{0.8}$ by the MCP is $2.36\mu_B$ which is in agreement with that of the above XMD result. (3) For Fe_3Pt the orbital moment is almost quenched and the spin moment is $6.8\mu_B$ which is corresponding to the value $6.68\mu_B$ by the magnetization measurement. (4) Directional anisotropy is observed for the three MCPs of $Pd_{3.2}Co_{0.8}$. These results are compared with the other experimental results such as polarized neutron diffraction [2] and the MCS. [3,4]

[1] B.J. Brown, *International Tables for Crystallography Vol. C* (Eds, A.J.C. Wilson and E. Prince, Kluwer Academic Publishers) **1999**, 450-457. [2] Y. Ito, T. Mizoguchi, *Solid State Commun.* **1974**, *15*, 807-809. [3] J.W. Taylor, J.A. Duffy, J. Poulter, A.M. Bebb, M.J. Cooper, J.E. McCarthy, D.N. Timms, J.B. Staunton, F. Itoh, H. Sakurai, B.L. Ahuja, *Phys. Rev. B* **2001**, *65*, 024442 1-7. [4] J.W. Taylor, J.A. Duffy, A.M. Bebb, J.E. McCarthy, M.R. Lees, M.J. Cooper, D. N. Timms, *Phys. Rev. B* **2002**, *65*, 224408 1-8.

Keywords: X-ray_magnetic_diffraction, magnetic_compton_ scattering, metallic alloy

MS48.P05

Acta Cryst. (2011) A**67,** C531

Perpendicular magnetic anisotropy in Co/Pd multilayer grown by MBE technique

Kosuke Suzuki,[a] Naoto Go,[a] Shun Emoto,[a] Masayoshi Itou,[b] Yoshiharu Sakurai,[b] Hiroshi Sakurai,[a] [a]*Departament of Production Science and Technology, Gunma University*, *Gunma (Japan).* [b]*Japan Synchrotron Radiation Research Institute*, *SPring-8, Hyogo (Japan).* E-mail: kosuzuki@gunma-u.ac.jp

Since discovery of high perpendicular magnetic anisotropy (PMA) in Co/Pd multilayer [1], they have attracted much attention for application to high density magnetic recording media. In order to achieve the high density recording, it is important to control the PMA energy in Co/Pd multilayer. It has been reported that the PMA energy in the Co/Pd multilayer depend on Pd layer thickness [2,3]. However the origin of these phenomena is unclear. The interface of the multilayer may affect the PMA energy. In this study we compare the two Co/Pd multilayers with smooth and rough interface.

A Co(1.5nm)/Pd(2.6nm) multilayer was grown on SiN membrane substrate by using effusion-cell of MBE technique. The deposition temperatures of Co and Pd were 1515°C and 1405°C, respectively. Deposition rates of Co and Pd were 0.5nm/min and 2nm/min, respectively. The XRD measurement showed fcc(111) texture and satellite peaks. The satellite peaks confirm the smooth interface.

The Co(1.6nm)/Pd(4.0nm) multilayer was grown by sputter technique previously [4]. The XRD measurement showed fcc(111) texture. Smaller satellite peak intensities suggest rougher interface than multilayer by the MBE.

Magnetization measurement showed that the PMA energy of the Co(1.5nm)/Pd(2.6nm) multilayer was 1.15×10^6erg/cc, and the Co(1.6nm)/Pd(4.0nm) multilayer was 1.2×10^6erg/cc. Two multilayers have almost the same PMA energy, even if the Co(1.5nm)/Pd(2.6nm) multilayer with the smooth interface has thinner Pd layer thickness.

In order to measure the shape of wave function in the two multilayers, magnetic Compton profiles (MCPs) were measured on BL08W of the SPring-8. Figure 1 shows MCPs for the Co(1.5nm)/ Pd(2.6nm) multilayer and Co(1.6nm)/Pd(4.0nm) multilayer. Both the MCPs are almost the same and it is suggested that wave function for the two multilayers are almost the same.

In conclusion we successfully control wave function and adjust the PMA energy by controlling the interface in Co/Pd multilayer.

[1] P.F. Carcia, A.D. Meinhaldt, A. Suna: *Appl. Phys. Lett.* **1985,** *47* 178-180. [2] H. Nemoto, Y. Hosoe: *J. Appl. Phys.* **2005,** *97,* 10J109 [3] P.F. Carcia: *J. Appl. Phys.* **1988,** *63*, 5066. [4] M.Ota: Gunma University master thesis **2006**, in Japanese.

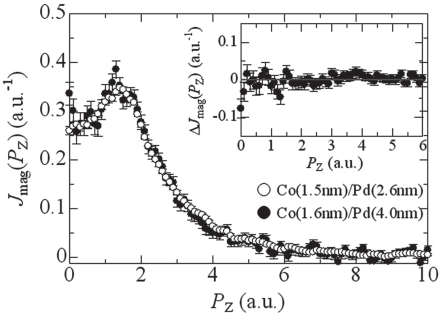

Fig.1 Magnetic Compton profiles (MCPs) of Co(1.5nm)/Pd(2.6nm) (open circles) and Co(1.6nm)/Pd(4.0nm) (solid circles) multilayers. The inset shows difference of the MCPs.

Keywords: multilayer, magnetic_compton_profile, magnetic_ anisotropy

MS49.P01

Acta Cryst. (2011) A**67,** C531-C532

Growth and characterization of selectively doped surface modified ZnO nanocrystals

K. Byrappa,[a] K. Namratha,[a] D. Ehrentraut,[b] G.K.L. Goh,[c] T. Adschiri,[d] [a]*Crystal Growth and Materials Science Laboratory, University of Mysore, Manasagangothri, (India).* [b]*World Premier International Research Center - Advanced Institute for Materials Research (WPI-AIMR), Tohoku University, (Japan),* [c]*Institute of Materials Research and Engineering, Agency for Science, Technology and Research, (Singapore).* [d]*Institute of Multidisciplinary Research for Advanced Materials, Tohoku University, (Japan).* Email: kbyrappa@gmail.com

ZnO nanocrystals find extensive application potential in modern technology for the fabrication of UV- diode laser and ZnO light emitting structures because of its wide and direct bandgap (3.37 eV) and with a large exciton binding energy (60 meV). ZnO has already been widely used in piezoelectric transducers, gas sensors, optical wave guides, transparent conductive films, varistors, solar cell windows, bulk acoustic wave devices, heterogeneous photocatalyst, etc. There are several methods employed popularly in the synthesis of ZnO nanocrystals. However, the hydrothermal method has been proved to be the most